Designer Spin Pseudomolecule Implemented with Trapped Ions in a Magnetic Gradient

A. Khromova, Ch. Piltz, B. Scharfenberger, T. F. Gloger, M. Johanning, A. F. Varón, and Ch. Wunderlich*

Department Physik, Naturwissenschaftlich-Technische Fakultät, Universität Siegen, 57068 Siegen, Germany

(Received 3 February 2012; published 1 June 2012)

We report on the experimental investigation of an individual pseudomolecule using trapped ions with adjustable magnetically induced J-type coupling between spin states. Resonances of individual spins are well separated and are addressed with high fidelity. Quantum gates are carried out using microwave radiation in the presence of thermal excitation of the pseudomolecule's vibrations. Demonstrating controlled-NOT gates between non-nearest neighbors serves as a proof-of-principle of a quantum bus employing a spin chain. Combining advantageous features of nuclear magnetic resonance experiments and trapped ions, respectively, opens up a new avenue toward scalable quantum information processing.

DOI: 10.1103/PhysRevLett.108.220502 PACS numbers: 03.67.Lx, 03.65.Ud, 37.10.Ty, 42.50.Dv

Successful experiments with molecules using nuclear magnetic resonance (NMR) [1–7] and with trapped ions [8–12] have been an important driving force for quantum information science. Early on during the development of quantum information science, NMR was successfully applied to carry out sophisticated quantum logic operations and complete quantum algorithms based on the so-called J-coupling between nuclear spins in molecules. In molecules used for NMR, the direct dipole-dipole interaction between nuclear spins is usually negligible. However, nuclear spins interact indirectly via J-coupling which is mediated by bonding electrons. This J-coupling provides a mechanism to implement conditional quantum dynamics with nuclear spins that are characterized by long coherence times and are manipulated using rf radiation. Scalability of NMR is hampered mainly by the use of ensembles of molecules making it difficult to prepare pure spin states. Also, nuclear spin resonances and J-coupling between spins in molecules are given by nature, and thus often are not well suited for quantum computing.

Here, effective spin-1/2 systems are realized by using long-lived hyperfine states of trapped atomic ions. The vibrational modes of this individual ion pseudomolecule [13] mediate an effective J-type coupling when exposing trapped ions to a spatially varying magnetic field [14–16]. The constants J_{ij} arising from magnetic gradient induced coupling (MAGIC) of such an individual spin-pseudomolecule can be adjusted through variation of the trapping potential that determines the frequencies ν_n of the ion crystal's vibrational modes. In addition, the range of interactions can be tuned by applying local static potentials [16,17]. Single spins can be addressed in frequency space, since the magnetic field gradient leads to a position dependent shift of an ion's resonance frequency [18,19]. A further useful feature of spin-pseudomolecules is the use of radio-frequency and microwave radiation for conditional quantum dynamics as opposed to laser light [18–21], a feature that substantially reduces experimental complexity and contributed to the rapid success of NMR in quantum information science. In addition, this eliminates spontaneous emission that otherwise may destroy coherences [22]. Moreover, J-type coupling in a spin-pseudomolecule is tolerant against thermal excitation of vibrational motion. This substantially reduces the necessity for cooling trapped ions in order to achieve high fidelity gates.

Exposing a trapped ion Coulomb crystal to a spatially varying magnetic field induces a spin-spin interaction mediated by the common vibrational motion of the ion crystal [14,15],

$$H = -\frac{\hbar}{2}\sum_{i<j}^{N} J_{ij}\sigma_z^{(i)}\sigma_z^{(j)}, \qquad (1)$$

where σ_z is a Pauli matrix and the coupling constants $J_{ij} = \sum_{n=1}^{N} \nu_n \kappa_{ni}\kappa_{nj}$. This sum extends over all vibrational modes with angular frequency ν_n, and $\kappa_{nl} \equiv \frac{\Delta z \partial_z \omega_l}{\nu_n} S_{nl}$ indicates how strongly ion l couples to the vibrational mode n, when the spin of ion l is flipped. Here, $\Delta z = \sqrt{\hbar/2m\nu_n}$ is the extension of the ground state wave function of vibrational mode n, and $\Delta z \partial_z \omega_l = g_F \mu_B b_l/\hbar$ gives the change of the ion's resonance frequency ω_l when moving it by Δz (b_l is the magnetic field gradient at the position of ion l, $\hbar$ is the reduced Planck's constant, μ_B the Bohr magneton, and g_F the Landé factor, e.g., $g_F = 1$ for $^{171}Yb^+$ ions in the electronic ground state). The dimensionless matrix elements S_{nl} give the scaled deviation of ion l from its equilibrium positions when vibrational mode n is excited. Such magnetic gradient induced coupling may also be implemented using electrons confined in a Penning trap [23]. Tunable spin-spin coupling based on optical dipole forces was proposed in [24] and demonstrated in [25,26].

After outlining how individual spins can be addressed with high fidelity in what follows, the measurement of the coupling matrix $\{J_{ij}\}$ for a three-spin–pseudomolecule is described. In addition, it is shown how coupling constants can be adjusted by variation of the ion trapping potential. Then, the experimental realization of controlled-NOT gates between any pair of spins is described, including a CNOT gate between non-neighboring ions. The entanglement of spins is proven by measuring the parity (defined below) of a two-spin state.

Hyperfine levels of the $^2S_{1/2}$ ground state of $^{171}\mathrm{Yb}^+$ serve as an effective spin-1/2 system [15], namely $|{\downarrow_i}\rangle \equiv {}^2S_{1/2}$ $(F = 0)$ and $|{\uparrow_i}\rangle \equiv {}^2S_{1/2}$ $(F = 1, m_F = +1)$, where $i = 1, 2, 3$ refers to ion i. These states are coherently controlled by microwave radiation near 12.65 GHz in resonance with the $|{\downarrow_i}\rangle \leftrightarrow |{\uparrow_i}\rangle$ transition. For the experiments presented here, we load three $^{171}\mathrm{Yb}^+$ ions in a linear Paul trap where the effective harmonic trapping potential is characterized by the secular radial frequency $\nu_r = 2\pi \times 502(2)$ kHz and axial frequency $\nu_1 = 2\pi \times 123.5(2)$ kHz. Initial preparation in state $|{\downarrow}\rangle$ is achieved by optical pumping on the $^2S_{1/2}$ $(F = 1) \leftrightarrow {}^2P_{1/2}$ $(F = 1)$ transition near 369 nm, and state-selective detection is done by registering resonance fluorescence scattered on the $^2S_{1/2}$ $(F = 1) \leftrightarrow {}^2P_{1/2}$ $(F = 0)$ electronic transition. This ionic resonance serves at the same time for Doppler cooling of the ion crystal. The population of the center-of-mass (c.m.) mode after Doppler cooling along the axial direction is $\langle n_1\rangle \approx 150$. Microwave sideband cooling is applied to attain $\langle n_1\rangle = 23(7)$ (details will be published elsewhere).

The ions are exposed to a magnetic field gradient along the z direction that is created by two hollow cylindrical SmCo permanent magnets plated with nickel and mounted at each end-cap electrode of the trap with identical poles facing each other. The total magnetic field amplitude is given by $B(z) = \sqrt{(B_{0\|} + b_{\mathrm{pm}} z)^2 + B_{0\perp}^2}$, where $B_{0\|} = 3.4 \times 10^{-4}$ T and $B_{0\perp} = 6.2 \times 10^{-5}$ T are longitudinal and radial components of the bias field at the coordinate origin defined by the position of the center ion, and $b_{\mathrm{pm}} = 19.0(1)$ T/m is the magnetic field gradient created by the permanent magnets in the absence of a perpendicular bias field. The magnetic field gradient $b_l = \partial_z B(z)|_{z=z_l}$ defined at the position z_l of ion l is smaller than b_{pm} and not constant due to the nonzero radial component $B_{0\perp}$ of the bias field.

The state $|{\uparrow}\rangle$ is magnetically sensitive and undergoes an energy shift $\Delta E = g_F \mu_B B$ due to the linear Zeeman effect, while state $|{\downarrow}\rangle$ to first order is insensitive to the magnetic field. Because of the gradient of the magnetic field, three ions with an inter-ion spacing of 11.9 μm [Fig. 1(a)] are subject to different energy shifts resulting in a frequency shift of the resonance $|{\downarrow}\rangle \leftrightarrow |{\uparrow}\rangle$ of approximately $\Delta f \simeq 3$ MHz between adjacent ions [Fig. 1(b)]. This energy shift makes it possible to address the ions independently in frequency space by using microwave radiation (or laser light [27]). The probability amplitude of exciting a neighboring ion decreases with the square of the detuning. Here, it is less than 4×10^{-4} (see Supplemental Material [28]).

In addition, the magnetic gradient induces the spin-spin interaction, Eq. (1), between the ions' internal states mediated by their common vibrational modes. Not only nearest neighbors interact but also the outer ions 1 and 3. The coupling constants J_{12}, J_{23}, and J_{13} have been measured in a Ramsey-type experiment and are displayed in Fig. 2(a) together with their calculated values. For these measurements, first all three ions are initialized in state $|{\downarrow\downarrow\downarrow}\rangle$. After a microwave $\pi/2$ pulse has been applied to ion j, this spin's precession will depend on the state of ion i which can be left in state $|{\downarrow_i}\rangle$ or set to $|{\uparrow_i}\rangle$ by a microwave π pulse. After time τ, a second $\pi/2$ pulse with variable phase ϕ is applied and the population $P(\phi)$ of $|{\uparrow_j}\rangle$ is measured with ion i initially prepared in state $|{\downarrow_i}\rangle$ or in $|{\uparrow_i}\rangle$, respectively. The coupling between ions i and j is then deduced from the phase difference $\Delta\phi_{ij}$ between these two sinusoidal signals $P(\phi)$: $J_{ij} = \Delta\phi_{ij}/2\tau$. In order to extend the coherence time of the spin states, which is limited by ambient magnetic field fluctuations, a multipulse spin-echo sequence is applied to ions i and j between the $\pi/2$-Ramsey pulses [28]. The third ion (labeled k) has no active role and is left in state $|{\downarrow_k}\rangle$ during the whole sequence. Its interaction with the other ions via J-coupling is canceled by the applied spin-echo sequence (which is true independent of its internal state).

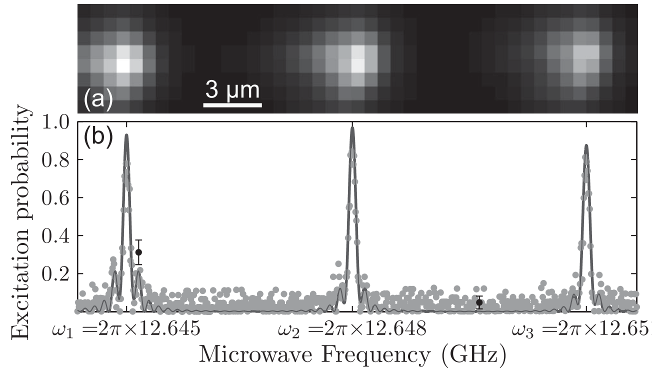

FIG. 1. Individual addressing of spins. (a) Spatially resolved resonance fluorescence (near 369 nm) of three $^{171}\mathrm{Yb}^+$ ions recorded with an intensified CCD camera is shown. Neighboring ions are separated by 11.9 μm. (b) Microwave-optical double resonance spectrum of the above ions. The spectrum was recorded by applying a microwave frequency pulse of 8 μs to the ions initially prepared in the state $|{\downarrow}\rangle$. The probability to find an ion in $|{\uparrow}\rangle$ was determined from counting resonance fluorescence photons while probing with laser light near 369 nm. In a magnetic gradient of ≈ 18.2 T/m, the qubit transitions $|{\downarrow}\rangle \leftrightarrow |{\uparrow}\rangle$ of different ions are nondegenerate. The solid line is a fit to the data. Each data point accounts for 50 repetitions. Two points with error bars are displayed representing the typical statistical standard deviations.

It is possible to encode quantum information in two sets of states, where one set is magnetically sensitive (as is used in this work), and the other set is not [e.g., $^2S_{1/2}$ $(F = 1, m_F = 0)$ and $(F = 0)$]. This allows for temporal storage of quantum information in magnetically insensitive states that do not couple to other spins and provide a memory intrinsically robust against ambient field fluctuations.

Figure 2(b) shows the dependence of J-type coupling on the c.m. frequency ν_1, that is, on the strength of the axial

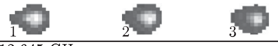

(a)

	1	2	3
1	12.645 GHz		
2	$2\pi\times32(4)$ Hz	12.648 GHz	
3	$2\pi\times18(2)$ Hz	$2\pi\times33(3)$ Hz	12.651 GHz

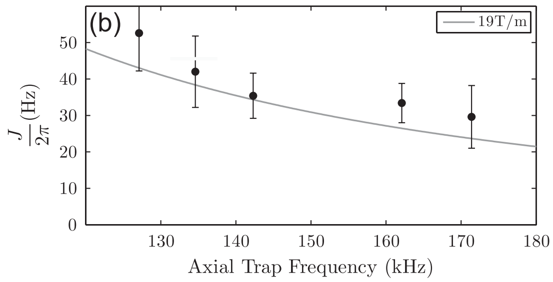

FIG. 2. J-type coupling of a three-spin pseudomolecule. In (a), the table lists the measured J-type coupling constants (below the diagonal) for a three-spin pseudomolecule together with the resonance frequencies of the microwave transitions (on the diagonal). For the nonuniform magnetic gradient present in our setup ($b_1 = 16.8$ T/m, $b_2 = 18.7$ T/m, $b_3 = 18.9$ T/m) and the axial trap frequency ($\nu_1 = 2\pi \times 123.5$ kHz), the calculated values are $J_{12} = 2\pi \times 32.9$ Hz, $J_{23} = 2\pi \times 37.0$ Hz, $J_{13} = 2\pi \times 23.9$ Hz. (b) Dependence of the coupling strength on the trapping potential. For a pseudomolecule consisting of two ions, the coupling strength J has been measured for varying c.m. frequency ν_1. A calculated curve for a uniform magnetic gradient of 19 T/m is represented by a solid line. These measurements demonstrate how J-type coupling can be varied by adjusting the trapping potential [16,17].

trapping potential. These data were taken with two trapped ions with the measurements carried out analogous to those described above, except that only a single spin-echo pulse was used here. This leads to shorter accessible precession times and thus smaller phase shifts which in turn yields a larger statistical error as compared to the data in Fig. 2(a). The data are in agreement with the calculated dependence of J on ν_1 ($J \propto (b/\nu_1)^2$).

J-type coupling between two spins is employed to implement a CNOT gate between ion 1 (control qubit) and ion 3 (target qubit). The evolution time $\tau = 11$ ms is chosen to achieve a phase shift of $\Delta\phi_{13} = \pi$. Figures 3(a) and 3(b) show the resulting state population of the target qubit as a function of phase ϕ of the last $\pi/2$-Ramsey pulse which is applied to the target qubit. The CNOT operation is achieved when selecting $\phi = 3\pi/2$. The four measured sets of data are in agreement with the truth table of the CNOT gate which induces a flip of the target qubit or leaves it unchanged depending on the initial state $|\uparrow\rangle$ or $|\downarrow\rangle$ of the control qubit.

The quantum nature of the conditional gate is verified by creation of entanglement in the outcome $|\psi_B\rangle = \frac{1}{\sqrt{2}} \times (|\downarrow_C\downarrow_2\downarrow_T\rangle + e^{i\alpha}|\uparrow_C\downarrow_2\uparrow_T\rangle)$ if the input is a superposition state. Only the correlations of the control and target qubit determine the parity $\Pi = P_{\uparrow\uparrow} + P_{\downarrow\downarrow} - (P_{\uparrow\downarrow} + P_{\downarrow\uparrow})$ of the resulting bipartite entangled Bell state (P_{ij}, $i, j = \downarrow, \uparrow$ denotes the probability to find the control and target qubits in the state $|ij\rangle$). When measuring in the σ_z basis, we observe a parity

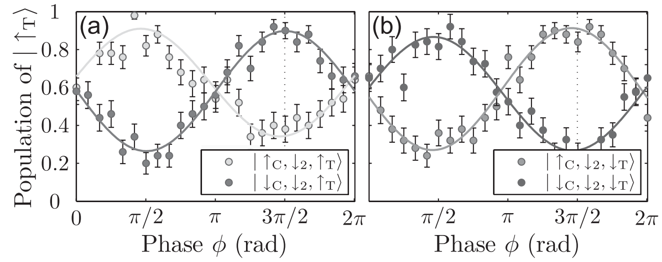

FIG. 3. Conditional quantum dynamics and CNOT gate between non-neighboring ions. The probability to find the target spin (ion 3) in state $|\uparrow\rangle$ at the end of a Ramsey-type sequence is shown as a function of the phase ϕ of the second $\pi/2$ pulse applied to the target. The inset shows the input state prepared before the Ramsey experiment. In (a) the target is initially prepared in $|\uparrow\rangle$ while in (b) it is prepared in $|\downarrow\rangle$. J-type coupling between the control qubit (ion 1) and the target qubit (ion 3) produces a phase shift on the target population as a function of the control qubit's state (different shades of gray). A free evolution time of $\tau = 11$ ms yields a phase shift of approximately π (3.1(2) radians) between the pairwise displayed curves. For $\phi = 3\pi/2$, a CNOT gate results. The middle ion, prepared in state $|\downarrow\rangle$, does not interact with other ions. Each data point represents 50 repetitions, the error bars correspond to mean standard deviations, and solid lines are fits to the data.

$\Pi_z = 0.43(13)$. To prove that the correlations are nonclassical, the parity $\Pi(\phi)$ was measured in addition along different bases [10] by applying additional $\pi/2$ pulses with phase ϕ to both ions. Figure 4 shows the resulting signal $\Pi(\phi)$ that oscillates with twice the phase variation, as one would expect for a bipartite entangled state. From the visibility of $V = 0.42(6)$ of the signal shown in Fig. 4 we evaluate the fidelity [10] of a Bell state $F = \frac{\Pi_z+1}{4} + \frac{V}{2}$ to be 0.57(4) which exceeds the Bell limit of 0.5 and thus proves the existence of entanglement. This shows that a conditional quantum gate between two non-neighboring ions is achieved.

In a similar manner, a CNOT gate was achieved between the first and the second ion with a fidelity of $F = 0.64(5)$ showing that it is possible to carry out on demand entangling operations between two ions at desired positions of the ion chain. For neighboring ions the coupling constants are higher, allowing for shorter evolution times (in this case 8 ms) and therefore reducing the effect of decoherence. In future experiments, microwave dressed states will be employed to extend the coherence time of magnetic sensitive states by several orders of magnitude [21], and thus the fidelity of quantum gates will be improved.

The entanglement procedure shown here can be applied to longer ion chains with minimal modifications. A large-scale quantum processor would be made up of an array of traps [11] each containing a spin-pseudomolecule allowing for simultaneous conditional quantum dynamics with more than two spins (multiqubit gates). This could substantially speed up the execution of quantum algorithms [29] and would be an alternative to a processor that contains zones for conditional quantum dynamics with two or three ions

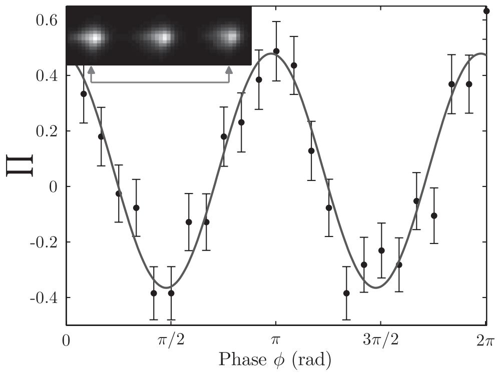

FIG. 4. Parity signal $\Pi(\phi)$ showing the quantum nature of the observed correlations of ion 1 and 3. The Bell state $|\psi_B\rangle = \frac{1}{\sqrt{2}} \times (|\downarrow_C\downarrow_2\downarrow_T\rangle + e^{i\alpha}|\uparrow_C\downarrow_2\uparrow_T\rangle)$ is the result of a CNOT operation applied to the superposition input state $|\psi_i\rangle = \frac{1}{\sqrt{2}}(|\downarrow_C\downarrow_2\downarrow_T\rangle + |\uparrow_C\downarrow_2\downarrow_T\rangle)$. In order to measure the correlations along different bases [10], microwave $\pi/2$ pulses with phase ϕ are applied to both ions followed by state-selective detection resulting in $\Pi(\phi)$ oscillating as $\cos(2\phi)$. The fidelity of creating the bipartite entangled state $|\psi_B\rangle$ is evaluated as $F = 0.57(4)$ (see text). Each data point represents 50 repetitions and error bars indicate 1 standard deviation.

[11]. Importantly, physical relocation (''shuttling'') of ions could be avoided during the processing of quantum information within a given spin-pseudomolecule [29]. The possibility to directly perform logic gates between distant qubits (e.g., the endpoints of a spin chain as demonstrated here) makes spin-pseudomolecules suitable as a quantum bus connecting different processor regions [30]. In that case, shuttling would be restricted to a pair of messenger ions which enable communication between different spin-pseudomolecules. In addition, a spin-pseudomolecule could serve as a versatile tool for quantum simulations of otherwise intractable physical systems [24–26,31,32].

It is desirable to increase the J-type constants due to MAGIC. This will be attained in microstructured ion traps [33,34] and trap arrays that allow for the application of larger magnetic gradients, or by using magnetic field gradients oscillating near the trap frequency [35]. In addition, segmented traps will allow for shaping J-coupling matrices by applying local electrostatic potentials [16,17], for example, to create cluster states [36], or to perform quantum simulations.

Assistance in data-taking by Th. Collath and D. Kaufmann and discussions with O. Gühne are gratefully acknowledged, as well as financial support by the Bundesministerium für Bildung und Forschung (FK 01BQ1012), Deutsche Forschungsgemeinschaft, and the European Commission under STREP PICC and iQIT.

*wunderlich@physik.uni-siegen.de

[1] D. G. Cory, A. F. Fahmy, and T. F. Havel, Proc. Natl. Acad. Sci. U.S.A. **94**, 1634 (1997).
[2] I. L. Chuang, L. M. K. Vandersypen, X. Zhou, D. W. Leung, and S. Lloyd, Nature (London) **393**, 143 (1998).
[3] J. A. Jones, M. Mosca, and R. H. Hansen, Nature (London) **393**, 344 (1998).
[4] R. Marx, A. F. Fahmy, J. M. Myers, W. Bermel, and S. J. Glaser, Phys. Rev. A **62**, 012310 (2000).
[5] E. Knill, R. Laflamme, R. Martinez, and C.-H. Tseng, Nature (London) **404**, 368 (2000).
[6] L. M. K. Vandersypen, M. Steffen, G. Breyta, C. S. Yannoni, M. H. Sherwood, and I. L. Chuang, Nature (London) **414**, 883 (2001).
[7] D. Suter and T. S. Mahesh, J. Chem. Phys. **128**, 052206 (2008).
[8] J. I. Cirac and P. Zoller, Phys. Rev. Lett. **74**, 4091 (1995).
[9] R. Blatt and D. Wineland, Nature (London) **453**, 1008 (2008).
[10] C. A. Sackett *et al.*, Nature (London) **404**, 256 (2000).
[11] D. Kielpinski, C. Monroe, and D. J. Wineland, Nature (London) **417**, 709 (2002).
[12] G. Kirchmair, J. Benhelm, F. Zähringer, R. Gerritsma, C. F. Roos, and R. Blatt, New J. Phys. **11**, 023002 (2009).
[13] D. J. Wineland, J. C. Bergquist, W. M. Itano, J. J. Bollinger, and C. H. Manney, Phys. Rev. Lett. **59**, 2935 (1987).
[14] Ch. Wunderlich, in *Laser Physics at the Limit*, edited by D. Meschede, C. Zimmermann, and H. Figger (Springer, New York, 2002), p. 261.
[15] Ch. Wunderlich and Ch. Balzer, Adv. At. Mol. Phys., **49**, 293 (2003).
[16] D. Mc Hugh and J. Twamley, Phys. Rev. A **71**, 012315 (2005).
[17] H. Wunderlich, Ch. Wunderlich, K. Singer, and F. Schmidt-Kaler, Phys. Rev. A **79**, 052324 (2009).
[18] F. Mintert and Ch. Wunderlich, Phys. Rev. Lett. **87**, 257904 (2001).
[19] M. Johanning, A. Braun, N. Timoney, V. Elman, W. Neuhauser, and Ch. Wunderlich, Phys. Rev. Lett. **102**, 073004 (2009).
[20] C. Ospelkaus, U. Warring, Y. Colombe, K. R. Brown, J. M. Amini, D. Leibfried, and D. J. Wineland, Nature (London) **476**, 181 (2011).
[21] N. Timoney, I. Baumgart, M. Johanning, A. F. Varón, M. B. Plenio, A. Retzker, and Ch. Wunderlich, Nature (London) **476**, 185 (2011).
[22] N. Akerman, S. Kotler, Y. Glickman, and R. Ozeri, arXiv:1111.1622v1.
[23] G. Ciaramicoli, F. Galve, I. Marzoli, and P. Tombesi, Phys. Rev. A **72**, 042323 (2005).
[24] D. Porras and J. I. Cirac, Phys. Rev. Lett. **92**, 207901 (2004).
[25] A. Friedenauer, H. Schmitz, J. T. Glueckert, D. Porras, and T. Schaetz, Nature Phys. **4**, 757 (2008).
[26] K. Kim, M. S. Chang, R. Islam, S. Korenblit, L.-M. Duan, and C. Monroe, Phys. Rev. Lett. **103**, 120502 (2009).
[27] S. X. Wang, J. Labaziewicz, Y. Ge, R. Shewmon, and I. L. Chuang, Appl. Phys. Lett. **94**, 094103 (2009).
[28] See Supplemental Material at http://link.aps.org/supplemental/10.1103/PhysRevLett.108.220502 for information about the experiment and its imperfections that presently limit the fidelity of conditional quantum gates.
[29] T. Schulte-Herbrüggen, A. Spörl, N. Khaneja, and S. J. Glaser, Phys. Rev. A **72**, 042331 (2005).

[30] D. Gottesman and I. L. Chuang, Nature (London) **402**, 390 (1999).
[31] Z. Li, M.-H. Yung, H. Chen, D. Lu, J. D. Whitfield, X. Peng, A. Aspuru-Guzik, and J. Du, Sci. Rep. **1**, 88 (2011).
[32] P. A. Ivanov and F. Schmidt-Kaler, New J. Phys. **13**, 125008 (2011).
[33] M. D. Hughes, B. Lekitsch, J. A. Broersma, and W. K. Hensinger, Contemp. Phys. **52**, 505 (2011).
[34] D. Kaufmann, T. Collath, M. T. Baig, P. Kaufmann, E. Asenwar, M. Johanning, and Ch.Wunderlich, arXiv:1107.4082 [Appl. Phys. B (to be published)].
[35] J. Welzel, A. Bautista-Salvador, C. Abarbanel, V. Wineman-Fisher, Ch. Wunderlich, R. Folman, and F. Schmidt-Kaler, Eur. Phys. J. D **65**, 285 (2011).
[36] H. J. Briegel, D. E. Browne, W. Dur, R. Raussendorf, and M. Van den Nest, Nature Phys. **5**, 19 (2009).